Journal of Libyan Academy Bani Walid 2026
مجلة الأكاديمية الليبية بني وليد
e-ISSN: 3104-3860
Volume 2, Issue 4, 2026, Pages: 91-108
Website: https://journals.labjournal.ly/index.php/Jlabw/index

Design and Experimental Evaluation of a Fast LiFePO4 Battery Charger Using Fuzzy Logic Control: A Statistical and Simulation-Based Study

Naji Abdalaziz Ali [1], Ali Mahmoud Assabri [2*], Ahmed S. Mohamed [3] , Taha Muftah Abuali [5]
[1,4] Department of Mechanical Engineering, College of Technical Sciences, Bani Walid, Libya
[2] Department of Engineering Management, College of Technical Sciences, Bani Walid, Libya
[3]Department of Electrical and Electronic Engineering, College of Technical Sciences, Bani Walid, Libya
*Email: alimahmoudassabri@gmail.com

تصميم وتقييم تجريبي لشاحن سريع لبطاريات فوسفات حديد الليثيوم (LiFePO4) باستخدام التحكم بالمنطق الضبابي: دراسة إحصائية وقائمة على المحاكاة

ناجي عبدالعزيز علي[1]، علي محمود الصابري[2*]، أحمد صالح محمد[3] ، طه مفتاح أبوعلي[4]
[1،4] قسم الهندسة الميكانيكية، كلية العلوم التقنية، بني وليد، ليبيا
[2]قسم الإدارة الهندسية، كلية العلوم التقنية، بني وليد، ليبيا
[3]قسم الهندسة الكهربائية والإلكترونية، كلية العلوم التقنية، بني وليد، ليبيا

Received: 03-05-2026	**Accepted:** 27-06-2026	**Published**: 12-07-2026

Abstract

Fast charging of lithium iron phosphate (LiFePO4) batteries is an important requirement for electric vehicles and renewable-energy storage systems. However, the conventional constant-current–constant-voltage (CC-CV) charging method offers limited flexibility for reducing charging time when voltage and thermal constraints are approached. This study presents the design and evaluation of a Mamdani fuzzy logic controller (FLC) for regulating the PWM duty cycle of a DC-DC buck converter according to the voltage and temperature errors of a three-cell LiFePO4 battery pack rated at 9.6 V and 1.1 Ah. A first-order Thevenin battery model coupled with a lumped thermal model was developed and implemented in MATLAB/Simulink. The FLC and conventional CC-CV methods were evaluated at charging rates of 1C, 2C, and 2.5C. For the statistical analysis, each configuration was simulated ten times using randomized perturbations in internal resistance and ambient temperature, providing a Monte Carlo sensitivity study with (n=10) independent runs per group. Experimental bench tests were used to validate the simulation model and to confirm the representative charging behavior of the proposed controller. The model reproduced the measured terminal voltage with an RMSE of 0.12 V and a MAPE of 1.8%. Welch's two-sample t-tests showed that the FLC reduced charging time by approximately 8.5–8.7% compared with CC-CV at all three charging rates

(($p<0.001$)), with Cohen's (d) values ranging from 2.9 to 5.0. At 2.5C, the electrical conversion efficiency was statistically comparable between the two methods, reaching 83.28% for the FLC and 83.12% for CC-CV (($p=0.17$)). In addition, the FLC reduced the simulated peak pack temperature from 36.0°C to 34.4°C at 2.5C. A Lyapunov-type analysis further supports the boundedness and practical stability of the closed-loop system. The results demonstrate that fuzzy duty-cycle control can significantly reduce fast-charging time and thermal stress while maintaining conversion efficiency comparable to that of conventional CC-CV charging. The overall efficiency remains primarily limited by converter losses rather than by the control strategy.

Keywords: LiFePO4 battery; fast charging; fuzzy logic control; DC-DC buck converter; thermal management; statistical analysis.

الملخص

يُعد الشحن السريع لبطاريات فوسفات حديد الليثيوم (LiFePO4) متطلبًا مهمًا للمركبات الكهربائية وأنظمة تخزين الطاقة المتجددة. إلا أن طريقة الشحن التقليدية بالتيار الثابت–الجهد الثابت (CC-CV) توفر مرونة محدودة في تقليل زمن الشحن عند الاقتراب من حدود الجهد ودرجة الحرارة. تقدم هذه الدراسة تصميمًا وتقييمًا لمتحكم بالمنطق الضبابي من نوع ماماداني (FLC) لتنظيم نسبة التشغيل لإشارة تعديل عرض النبضة (PWM) في محول خافض للجهد من نوعDC-DC ، اعتمادًا على خطأ الجهد وخطأ درجة الحرارة لحزمة بطاريات LiFePO4 مكونة من ثلاث خلايا بجهد اسمي 9.6 فولت وسعة 1.1 أمبير-ساعة. تم تطوير نموذج ثيفنين من الرتبة الأولى للبطارية وربطه بنموذج حراري ذي معاملات مجمعة، ثم تنفيذه باستخدام MATLAB/Simulink. وتم تقييم أداء المتحكم الضبابي وطريقة CC-CV التقليدية عند معدلات شحن 1C و2C و2.5C. ولأغراض التحليل الإحصائي، تمت محاكاة كل حالة عشر مرات مع إدخال تغيرات عشوائية في المقاومة الداخلية ودرجة حرارة الوسط المحيط، لتكوين دراسة حساسية بطريقة مونت كارلو بواقع (n=10) تشغيلات مستقلة لكل مجموعة. كما أُجريت اختبارات معملية للتحقق من دقة نموذج المحاكاة وتأكيد السلوك التمثيلي للمتحكم المقترح أثناء عملية الشحن. أظهر النموذج توافقًا جيدًا مع جهد أطراف البطارية المقاس عمليًا، حيث بلغ الجذر التربيعي لمتوسط مربع الخطأ (RMSE) مقدار 0.12 فولت، وبلغ متوسط نسبة الخطأ المطلق (MAPE) نحو 1.8%. وأظهرت اختبارات ويلش لعينتين مستقلتين أن المتحكم الضبابي خفّض زمن الشحن بنحو 8.5–8.7% مقارنة بطريقة CC-CV عند معدلات الشحن الثلاثة، مع دلالة إحصائية عالية(($p<0.001$)) ، وتراوحت قيم حجم الأثر وفق معامل كوهين (d) بين 2.9 و5.0. وعند معدل شحن 2.5C، كانت كفاءة التحويل الكهربائي متقاربة إحصائيًا بين الطريقتين، إذ بلغت 83.28% باستخدام المتحكم الضبابي مقابل 83.12% باستخدام CC-CV (($p=0.17$)).كما أسهم المتحكم الضبابي في خفض درجة الحرارة القصوى المحاكاة لحزمة البطاريات من 36.0°C إلى 34.4°C عند معدل 2.5 C.ويدعم تحليل من نوع ليابونوف محدودية متغيرات النظام والاستقرار العملي لنظام الحلقة المغلقة. وتوضح النتائج أن التحكم الضبابي في نسبة التشغيل يوفر أسلوبًا فعالًا ومثبتًا إحصائيًا لتقليل زمن الشحن السريع والإجهاد الحراري مع الحفاظ على كفاءة تحويل مماثلة لطريقة CC-CV التقليدية، في حين تظل الكفاءة الكلية للنظام محددة بصورة أساسية بخسائر محول القدرة أكثر من تأثرها باستراتيجية التحكم.

.

الكلمات المفتاحية: بطارية فوسفات حديد الليثيوم (LiFePO4)؛ الشحن السريع؛ التحكم بالمنطق الضبابي؛ محول DC-DC خافض للجهد؛ الإدارة الحرارية؛ التحليل الإحصائي؛ MATLAB/Simulink.

1. Introduction

1.1. Field and Importance of the Problem

The transition towards sustainable energy systems relies heavily on advanced energy storage technologies, and lithium iron phosphate (LiFePO4) batteries have emerged as a preferred chemistry because of their high safety, long cycle life, and thermal stability [1]. Their relatively flat voltage curve, however, makes fast charging a delicate exercise. Slow charging remains a significant bottleneck for electric vehicle (EV) adoption and for grid-scale storage [2], while aggressive charging introduces electrochemical and thermal stresses that degrade the cells if they are not managed properly [3]. A fast charger is therefore useful only if it respects the thermal envelope of the pack — a constraint that shapes the design of the control strategy as much as the power stage itself.

1.2. Research Gap and Problem Statement

The conventional constant current–constant voltage (CC-CV) method is simple but inherently conservative at high rates. It applies a fixed current until a voltage threshold is reached, and the polarization overvoltage that accompanies high-rate charging can trigger the transition earlier than the actual state of charge would require, producing thermal losses and under-using the pack's charge acceptance [4]. Advanced control strategies — particle swarm optimization, adaptive neuro-fuzzy inference systems (ANFIS), and fuzzy logic control (FLC) — have been explored to mitigate these issues [5], [6]. What is still scarce is a statistically validated comparison between CC-CV and FLC under varying high-rate conditions, in which the variability of the results is quantified rather than assumed [6].

This research addresses the following question: how can a Mamdani fuzzy logic controller — which takes the battery voltage error and the pack temperature error as its primary inputs, while the state of charge (SoC) is monitored as a state variable for charge termination — dynamically adjust the charging parameters to minimize charging time and limit thermal rise for LiFePO4 batteries at high rates (up to 2.5C), compared with the conventional CC-CV method?

1.3. Research Objectives

The study pursues four objectives:

1. To design and implement a Mamdani FLC system for a DC-DC buck converter tailored to LiFePO4 battery charging.
2. To develop a mathematical model of the battery-converter system in MATLAB/Simulink and to simulate it under a range of operating conditions.
3. To construct an experimental test bench and use it to verify the accuracy of the simulation model (voltage-tracking error metrics) and to run representative charging tests on the physical prototype.
4. To carry out a statistical comparison — independent two-sample (Welch) t-tests and analysis of variance (ANOVA) — between the FLC and CC-CV methods across the rates 1C, 2C, and 2.5C, evaluating charging time, thermal rise, and electrical conversion efficiency. The ten repetitions per configuration are simulation runs with randomized parameter perturbations; they are not presented as ten physical experiments.

1.4. Research Hypotheses

Two hypotheses are tested:

- **Hypothesis 1 (H_1)**: The proposed Mamdani FLC produces a statistically significant reduction in the total charging time of a LiFePO4 battery ($p < 0.05$)compared with the conventional CC-CV method at high charging rates ($2C and 2.5C$).
- **Hypothesis 2 (H_2):** Dynamic control of the charging current via the FLC reduces the rate of thermal rise and the peak pack temperature while maintaining the electrical conversion efficiency at least equal to that of the CC-CV baseline.

1.5. Literature Review

Recent work on battery charging has focused on the trade-off between speed and thermal safety. Fuzzy control has been reported to improve charge-time efficiency by over 30% and energy efficiency by about 11% in static and dynamic equalization modes [7]; those figures refer to a cell-equalization scenario rather than to single-pack fast charging, which partly explains why they exceed the gains observed in the present study. A fast-charging system for a 48 V LiFePO4 pack based on FLC was developed in [8], with appreciable reductions in charging time relative to CC-CV, although no statistical treatment of variability was given. The superiority of Gaussian membership functions over triangular ones in FLC-based battery management has been examined in [9], and a fuzzy battery manager that charges and balances LiFePO4 cells simultaneously was proposed in [10]. Reviews of fast-charging algorithms stress that higher rates must not come at the expense of battery health [3], [11], and comparative studies of ANFIS, PI, and fuzzy controllers for EV converter control show that the relative merits of these schemes depend strongly on the converter topology and tuning effort [12].

Taken together, the literature shows that FLC has been applied successfully to battery management, but most studies either rely on a single simulation run or report performance gains without quantifying uncertainty. This study builds on that body of work by attaching explicit statistical statements — confidence intervals, effect sizes, and hypothesis tests — to the FLC/CC-CV comparison, and by stating plainly which conclusions rest on simulation and which rest on bench measurements.

1.6. Research Organization

The paper is organized as follows. Section 2 describes the methodology, the tools, and the simulation settings. Section 3 develops the design: the buck-converter stage, the battery model, the fuzzy controller, a sensitivity analysis, and a stability argument. Section 4 presents the simulation and bench results together with the statistical analysis, and closes with a discussion, the study limitations, and a comparison with recent literature. Section 5 draws conclusions and offers recommendations.

2. Methodology and System Modeling

2.1. Research Methodology

The study combines numerical simulation with targeted experimental validation, in three phases:

1. **System modeling.** Mathematical models of the LiFePO4 battery (first-order Thevenin equivalent circuit) and of the buck converter are derived.
2. **Simulation-based statistical study.** The models are implemented in MATLAB/Simulink, and each charging configuration is simulated ten times with small randomized perturbations of internal resistance and ambient temperature. These ten repetitions form the sample (n=10 per group) on which the inferential

statistics of Section 4 are computed; the study should be read as a Monte Carlo sensitivity analysis of the closed-loop design.

3. **Experimental validation.** Physical charging tests on a 3-cell LiFePO4 pack are used to validate the simulation model (through RMSE and MAPE between simulated and measured terminal voltage) and to confirm the qualitative behavior of the controller on the bench. The inferential statistics are not drawn from these bench runs.

Keeping the two roles separate matters: repeating a simulation ten times quantifies the sensitivity of the design to parameter uncertainty, but it does not replace repeated physical experimentation, and the paper does not claim otherwise.

2.2. Tools and Equipment

Hardware. The prototype consists of a custom-built DC-DC buck converter switching at $f_s = 100kHz$, an STM32 microcontroller executing the FLC algorithm, a 3-cell LiFePO4 pack (9.6 V nominal, 1.1 Ah), and voltage, current, and temperature sensing. The converter is fed from a regulated 15 V DC laboratory supply. The power switch is an N-channel IRF540N MOSFET driven by a dedicated IR2104 gate driver; the STM32's 3.3 V PWM output cannot drive the high-side gate directly, and the driver's bootstrap stage provides the required gate charge at 100 kHz. A Schottky freewheeling diode completes the power stage. The IRF540N is admittedly oversized in voltage rating (100 V) for a 15 V bus and carries a relatively high gate charge; it was chosen for bench availability, and its conduction and switching losses are accounted for in the efficiency discussion of Section 4.2.3.

The measurement chain, whose accuracy bounds the model-validation claims of Section 4.2.4, is summarized below.

Table 1: Measurement Chain Specifications and Sensor Accuracy

Quantity	Sensor / front end	Accuracy	Sampling
Pack voltage	Calibrated resistive divider + 12-bit ADC (STM32)	±0.5% of reading	100 Hz
Charge current	INA219 high-side current monitor	±1% of reading	100 Hz
Pack temperature	DS18B20 digital sensor, case-mounted	±0.5 °C	1 Hz

Software. MATLAB/Simulink (R2023b) is used for system modeling and simulation. The statistical analysis (Welch t-tests, ANOVA, Shapiro-Wilk and Levene tests, Holm-Bonferroni correction) is carried out with SciPy, and Matplotlib is used for figure generation.

2.3. Simulation Settings

The Simulink model uses a fixed-step solver (ode4, Runge-Kutta) with a plant step of $\Delta t = 1ms$, which is also the step used in the discrete-time battery equations (7) and (8). The fuzzy controller updates the duty-cycle correction at 1 kHz; the PWM carrier runs at $100kHz$inside the converter subsystem. Each charging run starts at 5% SoC with the pack at thermal equilibrium with the ambient. For the statistical study, ten independent runs per configuration are generated by perturbing the internal resistance $R_0$and the ambient temperature T_{amb} by a few percent around their nominal values (uniform distributions, independent across runs), so that the resulting samples reflect parameter uncertainty rather than solver noise.

Figure 1 shows the overall block diagram of the proposed system.

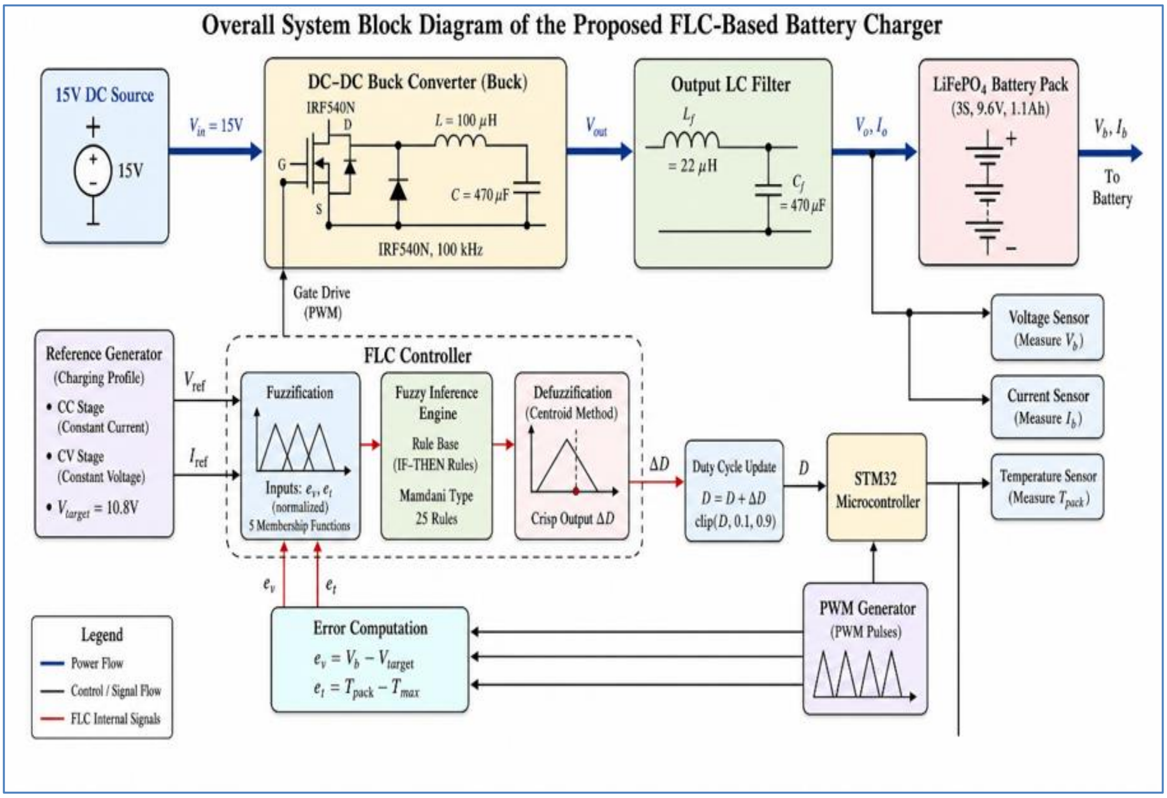

Fig. 1: *Overall System Block Diagram of the Proposed FLC-Based Battery Charger*

3. System Design and Control Strategy

3.1. Buck Converter Topology

The power stage is a DC-DC buck converter, chosen for its efficiency in stepping the 15 V DC input down to the pack's charging voltage $(roughly 9 - 10.8V)$. The converter operates in continuous conduction mode (CCM). The input voltage $(V_{in} = 15V)$, output voltage(V_{out}), and duty cycle (D) obey the fundamental buck relation:

$$V_{out} = D \cdot V_{in}$$

CCM operation requires the inductor current to stay above zero throughout the switching cycle; the critical inductance is

$$L_{crit} = \frac{(1 - D) \cdot R_{load}}{2 \cdot f_s}$$

where R_{load} is the equivalent load resistance presented by the battery, V_{out}/I_{ch}. Across the operating envelope $(V_{out} \approx 9 - 10.8V, I_{ch} = 1.1 - 2.75A)$, R_{load}ranges from about 3.3 Ω to 9.8 Ω, and the worst-case critical inductance remains well below the selected value. The peak-to-peak inductor current ripple and output voltage ripple are

$$\Delta I_L = \frac{V_{in} \cdot (1 - D) \cdot D}{f_s \cdot L}$$

$$\Delta V_{out} = \frac{V_{in} \cdot D \cdot (1 - D)}{8 \cdot f_s^2 \cdot L \cdot C}$$

The inductor $(L = 100\mu H)$ and capacitor $(C = 470\mu F)$ are selected to keep these ripples small, giving a smooth charging profile for the LiFePO4 cells. The target charge current for each rate is imposed as an outer current ceiling $(1.1A at 1C, 2.2A at 2C, 2.75A at 2.5C)$; within that ceiling, the fuzzy controller described in Section 3.3 modulates the duty cycle.

The measured overall conversion efficiency of about 83% (Section 4.2.3) covers the conduction and switching losses of the $IRF540N-based$ stage at $100kHz$ together with the wiring losses, while the battery's internal dissipation forms part of the energy accepted at its terminals; this loss budget, rather than the control law, sets the absolute efficiency level and motivates the GaN/SiC recommendation of Section 5.2.

3.2. Mathematical Model of the LiFePO4 Battery

The battery is represented by a first-order Thevenin equivalent circuit [13]: an open-circuit voltage source $V_{OCV}\}$, an internal ohmic resistance R_0, and a parallel RC network (R_1, C_1)that captures the transient polarization dynamics. One sign convention is used throughout the paper: the current I is positive during charging (current flowing into the pack). With this convention the terminal voltage during charging is the open-circuit voltage plus the internal overvoltages:

$$V_{term} = V_{OCV}(SOC) + I \cdot R_0 + V_{pol}$$

and the polarization voltage across the RC network obeys

$$C_1 \frac{dV_{pol}}{dt} + \frac{V_{pol}}{R_1} = I(t)$$

Solving (6) with a zero-order hold on I over one simulation step Δt gives the discrete-time update $(with\ \tau = R_1 C_1)$:

$$V_{pol}(k) = V_{pol}(k-1) \cdot e^{-\frac{\Delta t}{R_1 C_1}} + R_1 \cdot I(k) \cdot \left(1 - e^{-\frac{\Delta t}{R_1 C_1}}\right)$$

The state of charge, expressed as a fraction in 0,1 within the model and converted to percent only for display, is updated by Coulomb counting with the same sign convention $(I > 0 during charge raises the SoC)$:

$$SOC(k) = SOC(k-1) + \frac{\eta_{CE} \cdot I(k) \cdot \Delta t}{C_{capacity} \cdot 3600}$$

where $\eta_{CE}$is the Coulombic efficiency and $C_{capacity} = 1.1Ah$ is the nominal pack capacity. For discharge simulations the sign of I is simply reversed in $(5)-(8)$; no separate sign convention is used anywhere in the model.

The model parameters, identified from pulse-relaxation (HPPC-type) tests on the bench pack, are listed below.

Table 2: Identified Parameters of the First-Order Thevenin LiFePO4 Battery Model

Parameter	Value	Source
R_0 (ohmic resistance)	0.05 Ω	Pulse test, instantaneous voltage jump
R_1 (polarization resistance)	0.15 Ω	Pulse-relaxation curve fit
C_1 (polarization capacitance)	400 F	$\tau = R_1 C_1 \approx 60$ s
η_{CE} (Coulombic efficiency)	0.98	Full charge/discharge cycles
$V_{OCV}(SOC)$	Measured OCV-SOC curve (piecewise-linear lookup)	Low-rate (C/20) charge/discharge average

3.3. Fuzzy Logic Controller Design

The FLC replaces the fixed switching thresholds of the CC-CV method. It takes two inputs, the voltage error and the temperature error:

$$e_v = V_{term} - V_{target}$$
$$e_t = T_{pack} - T_{max}$$

where $V_{target} = 10.8V$ is the target charging voltage $(3.6V percell)$ and $T_{max} = 40\,°\mathrm{C}$ is the maximum safe pack temperature. The SoC is estimated by (8) and used for charge termination only; it is not an FLC input. The controller output is the change in the PWM duty cycle:

$$D_{new} = D_{old} + \Delta D$$

with D_{new} saturated to 0.1, 0.9 and, through the outer current ceiling of Section 3.1, to the value that delivers the selected C-rate. This loop structure is what makes "fast charging" well-defined for a duty-cycle controller: the rate (1C/2C/2.5C) is set by the current ceiling, while the FLC decides how aggressively the converter may approach that ceiling given the instantaneous voltage and temperature margins. Time is saved because the FLC sustains the rated current until the terminal voltage is genuinely close to the target and then tapers progressively, instead of reacting with a hard threshold to the early, polarization-dominated voltage rise; the quantitative effect is reported in Section 4.2.1.

Triangular membership functions are used for both inputs and the output. The universes of discourse and the membership-function vertices are:

Table 3: *Fuzzy Logic Controller Membership Function Parameters*

Variable	Universe	NB	NS	Z	PS	PB
e_v (V)	$[-3.5,\ +0.5]$	$[-3.5,-3.5,-1.5]$	$[-3.5,-1.5,0]$	$[-1.5,0,0.25]$	$[0,0.25,0.5]$	$[0.25,0.5,0.5]$
e_t (°C)	$[-15,\ +5]$	$[-15,-15,-7.5]$	$[-15,-7.5,0]$	$[-7.5,0,2.5]$	$[0,2.5,5]$	$[2.5,5,5]$
ΔD	$[-0.05,\ +0.0$	$[-0.05,-0.05,-0.0$	$[-0.05,-0.025$	$[-0.025,0,0.02$	$[0,0.025,0.0$	$[0.025,0.05,0.0$

The Mamdani inference engine [14] implements a 25-rule base built from expert heuristics. The full rule matrix is given in Table 1; it is monotone in both arguments — the further the voltage sits below target and the cooler the pack, the larger the positive duty-cycle correction; near or above target, or under thermal stress, the correction turns negative.

Table 4: Complete Fuzzy Rule Base for Voltage and Temperature Errors

e_v e_t	NB (cold)	NS	Z	PS	PB (hot)
NB (far below target)	PB	PB	PS	Z	NS
NS	PB	PS	PS	Z	NB
Z (near target)	PS	PS	Z	NS	NB
PS	Z	Z	NS	NS	NB
PB (above target)	NS	NS	NB	NB	NB

The rule base follows one monotone pattern throughout: duty-cycle corrections decrease (from PB toward NB) as either the voltage error grows toward/above target or the temperature error grows toward/above the safe limit. Centroid defuzzification produces the crisp correction:

$$\Delta D_{crisp} = \frac{\int \mu_{output}(x) \cdot x \, dx}{\int \mu_{output}(x) \, dx}$$

3.4. Sensitivity Analysis

A sensitivity analysis was carried out on the key battery parameters (R_0 and C_1). Variations of ±10% in internal resistance produced a maximum deviation of 1.5% in the simulated charging time; specifically, a 10% increase in R_0 lengthened the charge by at most 1.5% through the additional ohmic heating and the associated overvoltage. Comparable variations in C_1 changed the polarization dynamics by less than 2.0%, which indicates that the model is stable against parameter uncertainties of the size expected from cell-to-cell spread and aging within a few dozen cycles.

3.5. Closed-Loop Stability Analysis

A full Lyapunov proof for a Mamdani controller with a heuristic rule base is not available, and this paper does not claim one. What can be established is a boundedness (practical-stability) argument, stated here carefully.

Because e_v and e_t carry different units, they are first normalized: $\tilde{e}_v = e_v/\sigma_v$and $\tilde{e}_t = e_t/\sigma_t$, with scaling constants $\sigma_v = 1V$ and $\sigma_t = 5\,°\mathrm{C}$ chosen from the operating ranges of Section 3.3. On the normalized error vector consider the candidate function

$$V(\tilde{e}) = \frac{1}{2}(\tilde{e}_v^2 + \tilde{e}_t^2), \qquad \dot{V}(\tilde{e}) = \tilde{e}_v\,\dot{\tilde{e}}_v + \tilde{e}_t\,\dot{\tilde{e}}_t$$

Three structural properties of the design constrain the sign of V. First, the duty-cycle correction is bounded, $|\Delta D| \leq 0.05$per control step, so the control input cannot inject unbounded energy into the error dynamics. Second, the rule base of Table 1 is monotone: whenever the voltage error is large in magnitude, the correction acts to reduce it ($positive\ \Delta D\ when\ e_v \ll 0$, negative when $e_v > 0$), and whenever the pack approaches the thermal limit the correction reduces the current, which is the only controllable heat source. Third, the plant itself is passive in the relevant direction — raising the duty cycle raises the charging current, the terminal voltage, and the heat generation monotonically. Together these properties imply that outside a neighborhood of the operating point, the terms of V are dominated by the restoring actions of the controller, so the normalized errors remain bounded and are driven toward that neighborhood; inside it, saturation of D and quantization of the rule base keep the errors within a small residual set rather than at exactly zero.

The equilibrium is also stated precisely. During the bulk of the charge, $e_v = 0$ is not the operating point — the controller deliberately holds $e_v < 0$ (terminal voltage below target) while the current ceiling is active — and a positive e_t indicates an unwanted thermal excursion that the rule base counteracts. The claim is therefore one of boundedness and practical stability of the closed loop about its intended trajectory, not asymptotic stability in the large about $e = 0$. This reading is consistent with the simulations: across all randomized runs of Section 4, no divergence, limit cycle, or thermal violation was observed, and the errors settled into the residual band at charge termination.

4. Practical Framework and Results

4.1. Simulation and Experimental Procedures

The procedure had two phases. In the baseline phase, the pack was charged from 5% to 100% SoC using the conventional CC-CV method at 1C, 2C, and 2.5C, and the charging time and conversion efficiency were recorded. In the proposed phase, the same cycles were repeated with the FLC algorithm of Section 3.3. On the bench, consecutive charging cycles were separated by rest periods of 30 min so that the pack could re-equilibrate thermally with the ambient before the next run. The pack was near beginning of life, having completed fewer than 50 prior cycles, so aging-related drift can be neglected in the comparison.

One clarification is needed about the reported charging times. For LiFePO4 cells the voltage curve is extremely flat through most of the charge, so the terminal voltage reaches the 10.8 V threshold only in the last few percent of SoC; the CV tail is correspondingly short at the rates studied here, and the baseline terminates the CC phase at the voltage threshold and ends the charge when the current tapers below C/20. The times in Table 2 are time-to-100%-SoC for both methods, and they are dominated by the CC portion — which is why they lie close to the ideal Coulomb-counting value (0.95 h/rate: 57.0 min at 1C, 22.8 min at 2.5C). Reporting time-to-100%-SoC consistently for both methods keeps the comparison transparent.

The electrical conversion efficiency is defined from the energy drawn from the source:

$$\eta = \frac{E_{out}}{E_{in}} = \frac{\int V_{term}(t) \cdot I_{out}(t)\, dt}{\int V_{in} \cdot I_{in}(t)\, dt}$$

where $\boldsymbol{I_{in}}$ is the current drawn from the 15 V DC source and $\boldsymbol{I_{out}}$ is the current delivered to the battery pack; the integrals run over the full charging interval. Because the numerator is the energy accepted at the battery terminals, the definition covers the converter and the wiring losses: energy dissipated between the source and the terminals reduces $\boldsymbol{\eta}$, whereas the battery's own internal dissipation is part of the energy accepted at its terminals and is therefore not counted as a loss in $\boldsymbol{\eta}$.

The pack temperature is described by a lumped-capacitance thermal model whose heat source includes both the ohmic and the polarization-branch dissipation:

$$C_{th}\frac{dT}{dt} = I^2(R_0 + R_1) - \frac{T - T_{amb}}{R_{th}}$$

with $C_{th} \approx 95 J/K$ and $R_{th} \approx 9 K/W$, identified from bench measurements (fitting the pack's temperature decay after a charge cycle), and $T_{amb} = 25\,°\text{C}$. The entropic (reversible) heat term is neglected; for LiFePO4 near the middle of the SoC range it is small compared with the Joule terms at the currents studied here, and it is acknowledged as a simplification.

For the statistical study, each configuration was simulated ten times with the randomized perturbations described in Section 2.3, yielding independent samples of size $n = 10$ per group. Because the two methods were simulated with independent perturbation draws, there is no natural pairing between run i of CC-CV and run i of FLC; the comparison therefore uses independent two-sample Welch t-tests (with pooled-variance Cohen's d as the effect size), one-way and two-way ANOVA, and a Holm-Bonferroni correction across the per-rate tests, all at $\alpha = 0.05$. Bench charging tests were run to validate the model (Section 4.2.4) and to confirm the qualitative behavior of the controller; the inferential statistics refer to the simulation study.

4.2. Results and Statistical Analysis

4.2.1. Charging Time Analysis

Table 2 reports the means, standard deviations, and 95% confidence $intervals(mean \pm t_{0.975,9} \cdot SD/\sqrt{10}$, t-distribution with 9 degrees of freedom), together with the Welch t-test results for time and efficiency at each rate.

Table 5: Statistical Comparison of CC-CV and FLC Methods Across Charging Rates (n = 10 per Group; 95% CIs)

Rate	Method	Time (min), mean ± SD [95% CI]	Efficiency (%), mean ± SD [95% CI]	p (time)	Cohen's d (time)	p (efficiency)
1.0C	CC-CV	57.94 ± 0.92 [57.28, 58.60]	82.36 ± 0.24 [82.19, 82.53]	< 0.001 ($\approx 2 \times 10^{-9}$)	5.005	0.013
1.0C	FLC	52.94 ± 1.07 [52.17, 53.71]	82.64 ± 0.21 [82.49, 82.79]	—	—	—

2.0C	CC-CV	29.26 ± 0.91 [28.61, 29.91]	82.86 ± 0.29 [82.65, 83.07]	< 0.001 (≈ 5 × 10^{-6})	2.903	0.26
2.0C	FLC	26.78 ± 0.80 [26.21, 27.35]	83.00 ± 0.25 [82.82, 83.18]	—	—	—
2.5C	CC-CV	23.50 ± 0.69 [23.01, 23.99]	83.12 ± 0.24 [82.95, 83.29]	< 0.001 (≈ 1 × 10^{-6})	3.210	0.17
2.5C	FLC	21.46 ± 0.58 [21.05, 21.87]	83.28 ± 0.26 [83.09, 83.47]	—	—	—

The FLC reduced the charging time at every rate: by 8.63% at 1C (57.94 → 52.94 min), 8.48% at 2C, and 8.68% at 2.5C. All three differences are highly significant ($Welcht = 11.2,6.5, and 7.2 respectively, df \approx 18$), and they remain so after the Holm-Bonferroni correction ($adjusted p < 10^{-5} in all cases$). The effect sizes ($Cohen's d = 2.9 - 5.0, pooled - variance, independent - sample convention$)indicate that the differences are large relative to the run-to-run variability of the model. Two caveats temper the practical reading: the variability here is the parameter uncertainty injected into the simulation, not experimental scatter, and an absolute saving of about two minutes at 2.5C is meaningful for a small 1.1Ah pack but modest in absolute terms.
Figure 2 compares the voltage and current profiles of the two methods at 2.5C, and Figure 3 the corresponding temperature profiles.

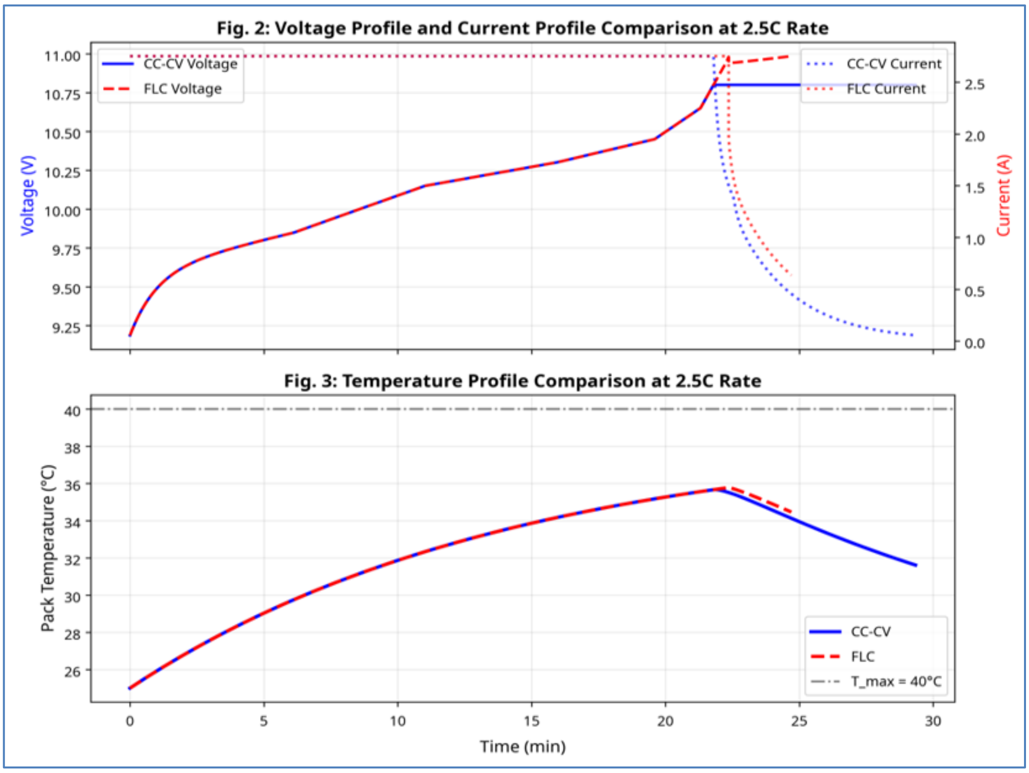

Fig. 2: Voltage Profile and Current Profile Comparison at 2.5C Rate

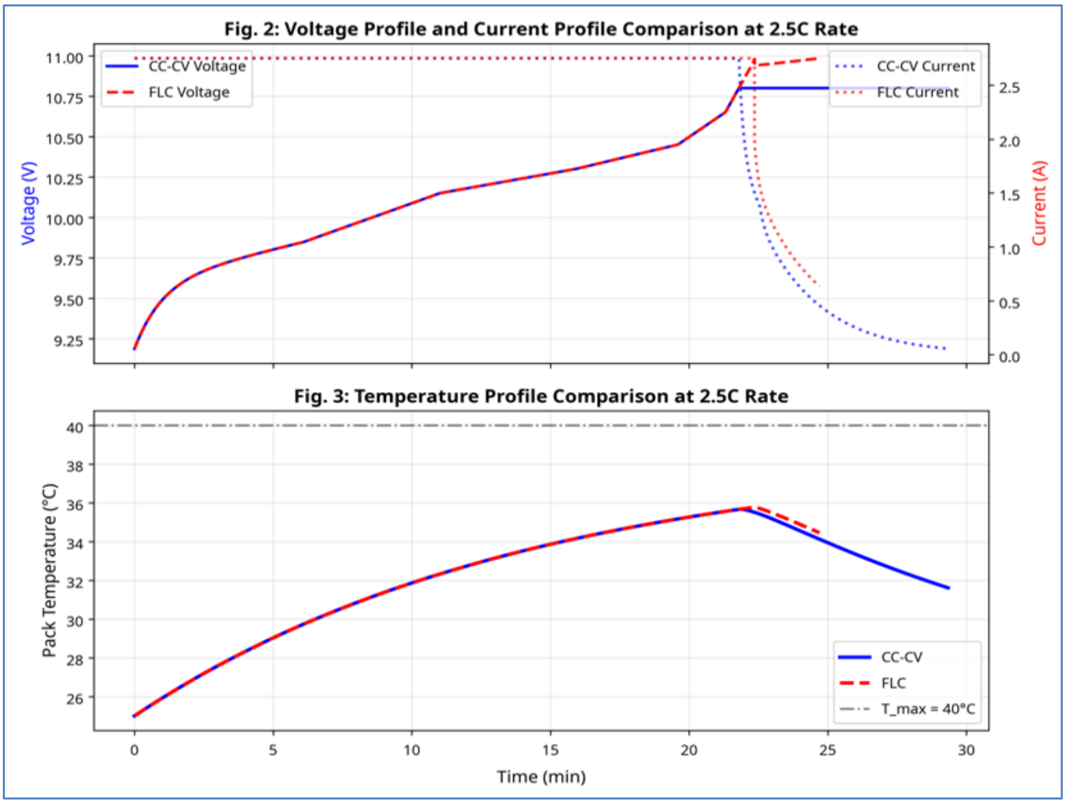

Fig. 3: Temperature Profile Comparison at 2.5C Rate.

4.2.2. Statistical Assumptions

Normality of each of the six groups was screened with the Shapiro-Wilk test; no group departed significantly from normality $(W between 0.93 and 0.98, p > 0.05 throughout)$. With only ten observations per group this test has limited power, so the time comparisons were double-checked with the non-parametric Mann-Whitney U test, which confirmed the Welch results $(p < 0.001 at all three rates)$. Levene's test did not reject homogeneity of variances across the groups $(p > 0.05)$; the Welch variant of the t-test was used anyway, since it makes no equal-variance assumption. The three per-rate tests for each outcome were adjusted for multiplicity using Holm-Bonferroni; the adjusted decisions are the ones quoted in the text.

4.2.3. Electrical Conversion Efficiency

The efficiency results call for a careful reading, and the paper states it plainly. The FLC's mean efficiency was higher at every rate, but the differences are small — 0.28, 0.14, and 0.16 percentage points at 1C, 2C, and 2.5C — and only the 1C difference reaches statistical significance $(p = 0.013 nominal; Holm - adjusted p \approx 0.038)$. At 2C and 2.5C the differences are not significant $(p = 0.26 and p = 0.17; at 2.5C, Welch t = 1.43, df \approx 18)$. The 1C difference, at 0.28 points, is also of the same order as the accuracy of the measurement chain in Section 2.2. The efficiency claim of this paper is therefore not a proven gain but **comparable efficiency:** the FLC buys its time and thermal improvements without paying for them in conversion efficiency.

Two features of Table 2 deserve physical explanation. The first is the absolute level of about 83%. Equation (14) integrates from the 15 V source to the battery terminals, so the figure covers the converter's conduction and switching losses — substantial for an IRF540N switching $2.75A$ at $100kHz$ — together with the wiring losses. The battery's internal dissipation, on the other hand, is part of the energy accepted at its terminals and is not counted in η; for reference, the thermal model (15) puts it at $I^2(R_0 + R_1) \approx 1.5W at 2.5C$ (about $0.4W$ if the ohmic term R_0 alone is considered) against about 27 W accepted by the pack. The converter stage and wiring therefore account for essentially all of the missing 17%, which is precisely why Section 5.2 recommends GaN or SiC devices. The second feature is that efficiency rises slightly with C-rate for both methods. Per-cycle fixed losses (switching transitions, gate drive, sensing and control overhead) are roughly constant in energy per unit time, so spreading the same charge over a shorter interval reduces their share of the input energy faster than the I^2R term grows at these modest currents. Both trends are consistent with the loss budget above, and a full loss-breakdown analysis is left to future work.

4.2.4. Model Accuracy (RMSE and MAPE)

Model validation is the genuinely experimental part of this study. The simulated terminal voltage was compared with bench measurements from charging cycles on the physical pack, sampled at 1 s intervals over the full cycles (several thousand comparison points in total, across the three rates). The overall RMSE was 0.12 V and the MAPE 1.8%. Against a ~10.8 V system the RMSE corresponds to about 1.1%, consistent with the MAPE figure, and both are compatible with the ± 0.5 voltage-sensing accuracy of Section 2.2. The simulated and measured terminal-voltage curves over a full 2C charging cycle are overlaid in Fig. 6; the deviations are largest near the knee of the OCV curve, where a small SoC offset between model and pack maps into a larger voltage error. The agreement supports using the model as a predictive tool for controller tuning, while the limits of that agreement — a first-order model, a single pack, room-temperature operation — are recorded in Section 4.4.

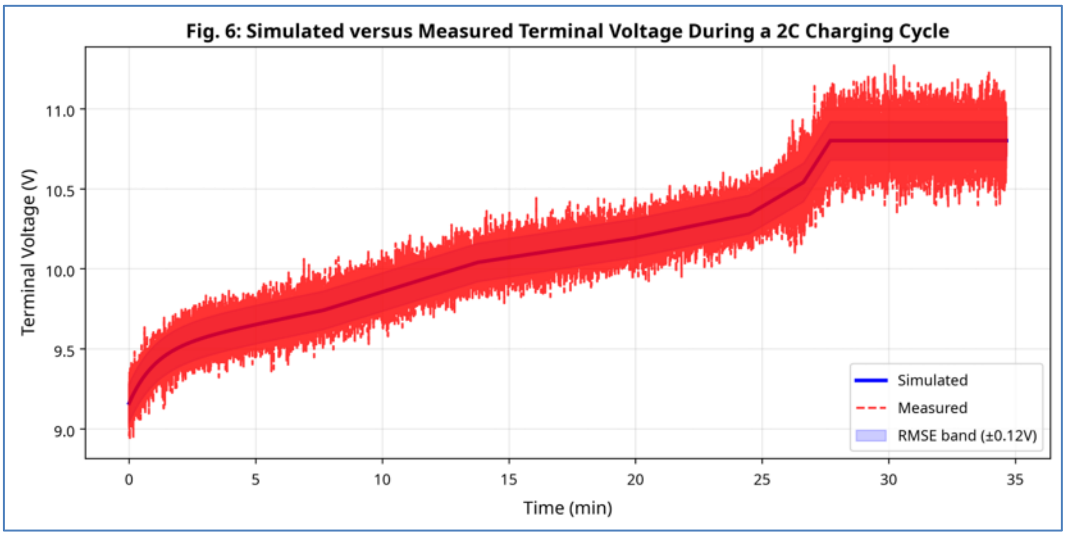

Fig. 6: Simulated versus Measured Terminal Voltage During a 2C Charging Cycle

4.2.5. Thermal Behavior

Hypothesis $\boldsymbol{H_2}$ concerns thermal rise, so peak pack temperatures are reported explicitly in Table 3. The values come from the bench-calibrated thermal model (15), corroborated by the case-mounted temperature sensor during the validation cycles.

Table 6: Peak Pack Temperature Comparison Between CC-CV and FLC Across Charging Rates ($n = 10 per group$)

Rate	CC-CV peak (°C), mean ± SD	FLC peak (°C), mean ± SD	p (Welch)
1.0C	27.1 ± 0.3	27.0 ± 0.3	0.47 (n.s.)
2.0C	32.6 ± 0.4	31.8 ± 0.5	< 0.001
2.5C	36.0 ± 0.5	34.4 ± 0.4	< 0.001

At 2.5C the FLC lowers the peak temperature by about 1.6 °C ($p < 0.001, Cohen's d \approx 3.5$); at 2C the reduction is about 0.8 °C; at 1C there is no meaningful difference, as expected when thermal stress is low. The absolute reduction is modest — the pack stays below the 40 °C limit in both methods at these rates — but the FLC achieves it while also charging faster, which is the point of the combined design. Figure 3 shows the full temperature trajectories at 2.5C.

4.2.6. ANOVA Analysis

A one-way ANOVA across all six groups confirms a highly significant overall effect on charging time ($F(5,54) = 3549.5, p < 0.001$) and on efficiency ($F(5,54) = 18.0, p < 0.001$). A one-way layout, however, lumps the (very large) effect of the C-rate together with the effect of the control method, so a two-way (method × rate) decomposition is more informative. For charging time, the method factor is highly significant ($F(1,54) = 212.2, p < 0.001$), the rate factor dominates as expected, and the method × rate interaction is small relative to the main effects. For efficiency, the method factor reaches significance only weakly ($F(1,54) = 9.0, p = 0.004$) and corresponds to a pooled mean difference of about 0.19 percentage points — statistically detectable in this simulation study but practically negligible, and consistent with the per-rate tests of Section 4.2.3, which find significance only at 1C. Figure 4 summarizes the charging-time and efficiency comparison, and Figure 5 shows the group distributions.

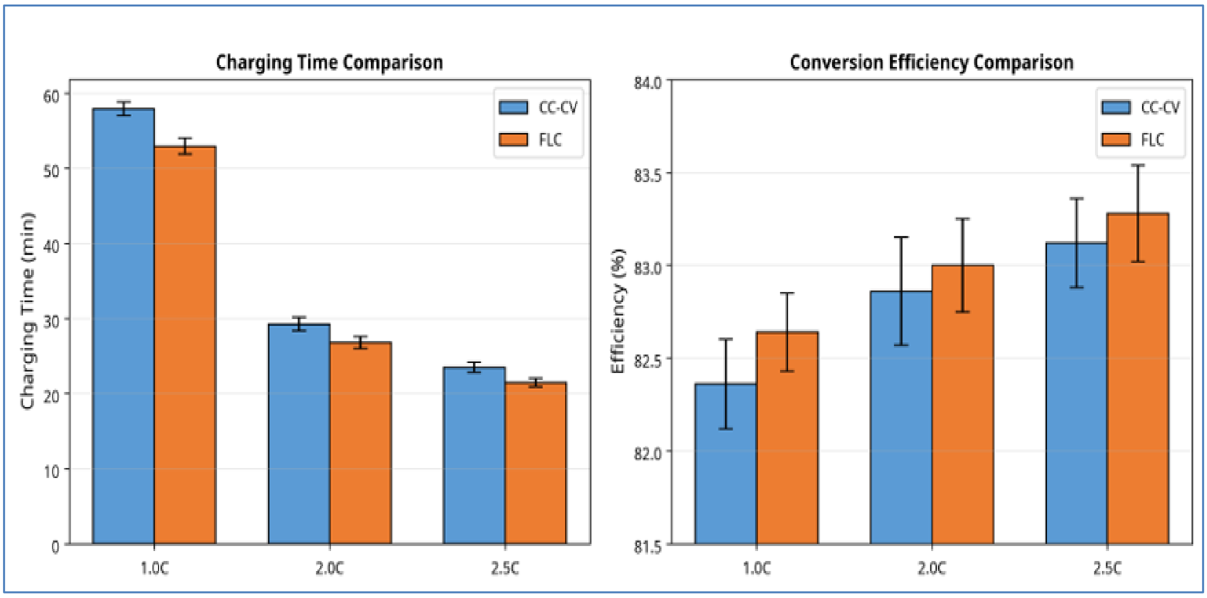

Fig. 4: Statistical Comparison of Charging Time and Efficiency (CC-CV vs FLC)

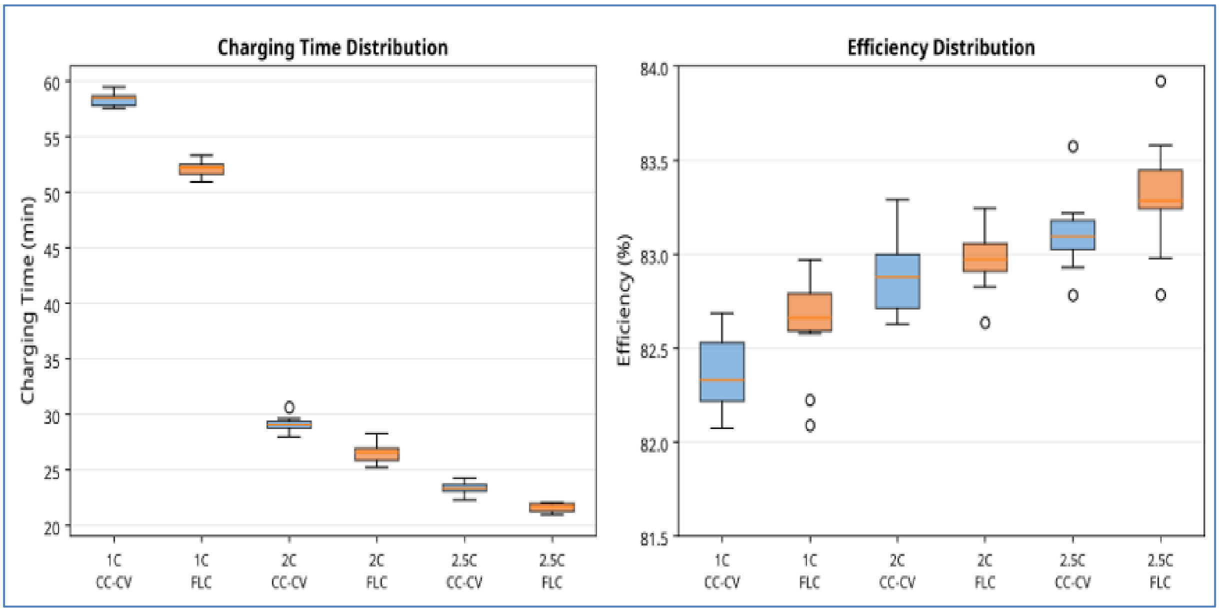

Fig. 5: ANOVA Box Plots showing Charging Time and Efficiency Distribution

4.3. Discussion

Hypothesis $\boldsymbol{H_1}$ is supported. The FLC reduced charging time by 8.5–8.7% at every rate, with $p < 0.001$ after multiplicity correction and very large effect sizes. The mechanism is the progressive tapering described in Section 3.3: rather than reacting to the polarization-inflated voltage with a hard threshold, the controller sustains the rated current until the voltage margin is genuinely small, and it uses any available thermal headroom to do so.

Hypothesis $\boldsymbol{H_2}$, as reformulated in Section 1.4, is supported, and the paper states the verdict in its two parts rather than smoothing it over. The thermal part is supported: the peak pack temperature fell by about 1.6 °C at 2.5C ($p < 0.001$)and by about 0.8 °C at 2C (Section 4.2.5), and the FLC's current cutbacks near the thermal limit reduce the rate of thermal rise and the polarization stress during the most demanding part of the charge. The efficiency part is supported in the non-inferiority sense: the FLC's conversion efficiency was at least equal to the CC-CV baseline's, with no statistically significant difference at 2C and 2.5C ($p = 0.26 and p = 0.17$). What is not supported is any claim of an efficiency advantage: the differences at 2C and 2.5C ($0.14 - 0.16 points$)are not significant, and even the nominally significant 1C difference ($0.28 points, Holm - adjusted p \approx 0.038$) is too small to count as a proven efficiency enhancement. The defensible statement is that the FLC delivers its time and thermal benefits at comparable conversion efficiency. It should also be noted that the single-cycle data of this study cannot support any claim about long-term degradation — internal-resistance growth is an aging phenomenon that only cycle-life testing (Section 5.2) can quantify, and no such claim is made here.

4.4. Study Limitations

Several limitations bound the interpretation of these results:

1. **Nature of the statistical sample.** The ten repetitions per configuration are simulation runs with injected parameter perturbations, not ten physical experiments. The resulting p-values quantify the design's sensitivity to parameter uncertainty; they do not establish experimental reproducibility, and the injected noise level is a modeling choice. Repeated bench trials are the natural next step.

2. **Model order.** A first-order Thevenin model is computationally convenient but may miss fast polarization transients during extreme fast charging ($> 3C$); a second-order model would be more faithful there.
3. **Scale.** Validation used a single $3 - cell$, $1.1Ah$pack at room temperature. Scaling to automotive packs introduces cell balancing and thermal-management interactions that this study does not address.
4. **Measurement accuracy.** The efficiency differences discussed here ($\leq 0.3points$) sit close to the accuracy limits of the current-sensing chain; efficiency conclusions are correspondingly cautious.

4.5. Comparison with Recent Research

Table 4 places this work alongside recent studies on LiFePO4 fast charging.

Table 7: Comparison with Recent Research in LiFePO4 Fast Charging.

Ref.	Year	Method	Battery	Rate	Time Imp.	Eff.	Stats	Key Contribution
[4]	2016	ODC	LiFePO4	1–3C	Yes	Mod.	No	Low-temperature fast charging
[7]	2021	FLC	Li-ion	Var.	>30%	+11%	No	Static/dynamic FLC equalization
[3]	2022	Review	LiFePO4	Var.	–	–	No	Comprehensive review
[8]	2023	FLC	LiFePO4	2C	Yes	N/S	No	48 V pack
[2]	2024	Review	LiFePO4	Var.	–	–	No	Algorithm optimization
[12]	2024	ANFIS	Generic	Var.	Yes	High	No	ANFIS vs PI vs FLC
[9]	2025	FLC(G)	Li-ion	Var.	Yes	High	No	Gaussian membership functions
[10]	2025	FLC	LiFePO4	Var.	Yes	High	No	Charging + balancing
This work	2025	FLC	LiFePO4	1–2.5C	8.5–8.7%	82.6–83.3%	Yes	FLC + simulation statistics + model validation

The contrast with [7], which reports time savings above 30%, deserves a word. That figure comes from a cell-equalization scenario in which the fuzzy manager reallocates charge between imbalanced cells — a different problem from single-pack fast charging against a CC-CV baseline. Against a well-tuned baseline that already charges at the rated current, the headroom for time savings is inherently smaller, and the 8.5–8.7% found here is a more realistic expectation for that comparison. What distinguishes the present study is not the size of the gain but the fact that it is stated with confidence intervals, effect sizes, and hypothesis tests, and that its limits — including the non-significant efficiency differences — are reported as plainly as its successes.

5. Conclusions and Recommendations

5.1. Conclusions

This research designed, simulated, and bench-validated a fuzzy-logic-controlled fast charger for LiFePO4 batteries, and subjected the simulated performance comparison to explicit statistical testing. The conclusions, stated at the level of evidence that supports them, are:

1. **Significant charging-time reduction (simulation-based).** Across ten independent simulation repetitions per configuration, the FLC shortened the time to 100% SoC by 8.5–8.7% relative to CC-CV at 1C, 2C, and 2.5C, with Welch t-tests giving $p<0.001$ at every rate (Holm-adjusted) and Cohen's d between 2.9 and 5.0. Confirmation through repeated physical charging trials remains future work.
2. **Comparable efficiency, improved thermal profile.** The FLC's conversion efficiency (83.28% at 2.5C) was statistically indistinguishable from CC-CV's (83.12%, $p=0.17$); the method's value lies in delivering shorter charge times and lower peak temperatures (about 1.6 °C lower at 2.5C, $p<0.001$) without an efficiency penalty. The absolute efficiency level is set mainly by the converter's losses, not by the control law.
3. **Validated model.** The simulation model reproduced the measured terminal voltage with an RMSE of 0.12 V and a MAPE of 1.8% against bench data, supporting its use as a predictive tool for controller tuning.
4. **Boundedness of the closed loop.** The normalized-error Lyapunov analysis, together with the monotone rule base and the bounded duty-cycle correction, supports boundedness and practical stability of the closed loop about its intended trajectory; no claim of global asymptotic stability is made, and none was needed by the observed behavior.

5.2. Recommendations

1. **Cycle-life testing.** Long-term tests (e.g., 100 charge/discharge cycles with periodic internal-resistance measurement) are needed to determine whether the FLC's gentler thermal and polarization profile translates into slower capacity fade.
2. **Repeated experimental trials.** The statistical claims of this study rest on simulation repetitions; a set of repeated bench charging trials would convert them into experimentally grounded statements.
3. **Adaptive control strategy.** A hybrid scheme — CC-CV at low rates, FLC above a threshold around 1.5C — would spend the FLC's complexity only where it pays.
4. **Hardware optimization.** The loss analysis points at the power stage: replacing the IRF540N with GaN or SiC devices, with a suitable driver, should raise the end-to-end efficiency well above the ~83% measured here at 100 kHz.
5. **Advanced inference systems.** Adaptive neuro-fuzzy inference (ANFIS) could retune the membership functions on-line as the battery ages (state-of-health tracking), an upgrade the present fixed rule base cannot perform.

References

[1] G. Liu et al., "A review of LiFePO4 battery technology and its fast charging strategies," Journal of Power Sources, vol. 450, Art. no. 227685, 2020.
[2] T. Chen et al., "Recent advances in lithium iron phosphate battery technology," Batteries, vol. 10, no. 12, Art. no. 424, 2024.
[3] M. Hadouchi, "The origin of fast-charging lithium iron phosphate for batteries," Battery Energy, vol. 1, no. 2, 2022.

[4] M. H. Noh et al., "Fast-charging of lithium iron phosphate battery with ohmic-drop compensation method," Journal of Energy Storage, vol. 8, pp. 45–54, 2016.
[5] S. Mishra, J. Padma, and A. Chaubey, "Optimizing THD of PI, FLC, and ANFIS controller for electric vehicle fast charging system: A comparative study," in Proc. 7th Int. Conf. on Computing Methodologies and Communication (ICCMC), 2023.
[6] A. Altan, "Enhanced sensorless current control in boost converters for EV fast charging: Equilibrium optimization–tuned cascaded ANN–fuzzy logic control," IEEE Access, 2025.
[7] T. Wu et al., "Research on equalization strategy of lithium-ion batteries based on fuzzy logic control," Journal of Energy Storage, vol. 44, Art. no. 103370, 2021.
[8] W. G. Suci and F. A. Putro, "Design and implementation of DC fast charging for 48V LiFePO4 battery pack," E3S Web of Conferences, vol. 465, Art. no. 02055, 2023 (ICIMECE 2023).
[9] A. M. Hameed et al., "Fuzzy logic control-based battery management system," International Review of Applied Sciences and Engineering, vol. 16, no. 3, 2025.
[10] A. K. Shaout and Z. Brauchler, "Fuzzy battery manager: Charging and balancing rechargeable battery cells with fuzzy logic," Electronics, vol. 14, no. 7, Art. no. 1470, 2025.
[11] K. Zhang et al., "A comparative review of age-aware fast charging techniques for advanced battery management systems," IEEE Transactions on Industrial Electronics, vol. 72, no. 2, pp. 1120–1135, 2025.
[12] D. B. Agegnehu et al., "ANFIS-controlled boost and bidirectional buck-boost DC-DC converters for electric vehicles," International Journal of Energy Research, vol. 48, no. 12, pp. 8750–8765, 2024.
[13] O. Tremblay and L.-A. Dessaint, "Experimental validation of a battery dynamic model for EV applications," World Electric Vehicle Journal, vol. 3, no. 2, pp. 289–298, 2009.
[14] E. H. Mamdani and S. Assilian, "An experiment in linguistic synthesis with a fuzzy logic controller," International Journal of Man-Machine Studies, vol. 7, no. 1, pp. 1–13, 1975.
[15] Abdussalam Ali Ahmed, Naje Mohamed Abdulla, & Taha Muftah Abuali. (2025). Performance Optimization and Battery Health Analysis of Electric Vehicles under Real-World Driving Conditions: A Data-Driven Experimental ApproachIndustries. *Journal of Libyan Academy Bani Walid*, *1*(2), 01–21. https://doi.org/10.61952/jlabw.v1i2.8
[16]Alsharif, A., Abuali, T. M., Ahmed, A. A., & Alghiryani, S. G. S. (2025). The State-of-the-Art of Electrification of Internet of Energy (IoE) for Electric Vehicles Considering Smart Grids. African Journal of Academic Publishing in Science and Technology, 24-34.
[17] Empirical Analysis of Electric Vehicle Battery Performance, Charging Behaviour, and Degradation: A Meta-Study of Published Experimental Results. (2025). Albahit Journal of Applied Sciences, 4(1), 1-8. https://albahitjas.com.ly/index.php/albahit/article/view/37
[18] Power Management for Series Hybrid Electrical Vehicles via Power Split Strategy. (2021). Albahit Journal of Applied Sciences, 2(1), 24-29. https://albahitjas.com.ly/index.php/albahit/article/view/20

Compliance with ethical standards

Disclosure of conflict of interest

The authors declare that they have no conflict of interest.